

## Sensitivity of Boron Nitride Nanotubes toward Biomolecules of Different Polarities

Saikat Mukhopadhyay,<sup>†</sup> Ralph H. Scheicher,<sup>‡</sup> Ravindra Pandey,<sup>\*,†</sup> and Shashi P. Karna<sup>\*,§</sup>

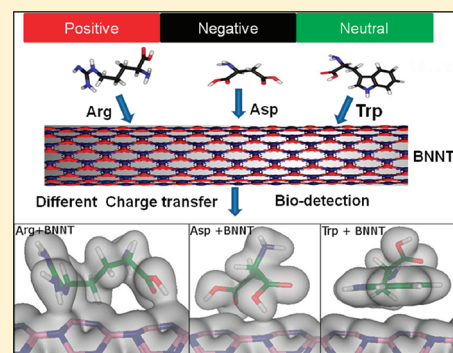
<sup>†</sup>Department of Physics, Michigan Technological University, Houghton, Michigan 49931, United States

<sup>‡</sup>Department of Physics and Astronomy, Uppsala University, SE-751 20 Uppsala, Sweden

<sup>§</sup>U.S. Army Research Laboratory, Weapons and Materials Research Directorate, ATTN: RDRL-WM, Aberdeen Proving Ground, Maryland 21005-5069, United States

**ABSTRACT:** The effect of molecular polarity on the interaction between a boron nitride nanotube (BNNT) and amino acids is investigated with density functional theory. Three representative amino acids, namely, tryptophane (Trp), a nonpolar aromatic amino acid, and aspartic acid (Asp) and arginine (Arg), both polar amino acids are considered for their interactions with BNNT. The polar molecules, Asp and Arg, exhibit relatively stronger binding with the tubular surface of BNNT. The binding between the polar amino acid molecules and BNNT is accompanied by a charge transfer, suggesting that stabilization of the bioconjugated complex is mainly governed by electrostatic interactions. The results show modulation of the BNNT band gap by Trp. Interestingly, no change in band gap of BNNT is seen for the polar molecules Asp and Arg. The predicted higher sensitivity of BNNTs compared to carbon nanotubes (CNTs) toward amino acid polarity suggests BNNTs to be a better substrate for protein immobilization than CNTs.

**SECTION:** Nanoparticles and Nanostructures



In recent years, bioconjugated nanostructured materials including nanotubes,<sup>1–5</sup> nanowires,<sup>6</sup> fullerenes,<sup>7</sup> and nanoparticles<sup>8,9</sup> have emerged as a new class of materials for biosensing and medical diagnostics applications. For example, DNA-decorated carbon nanotubes were shown to be effective for chemical sensing of various odors.<sup>10</sup> On the other hand, probing of conformational changes in DNA *in vivo* triggered by a change in the surrounding ionic concentration showed a great possibility for new detection mechanism.<sup>11</sup> Conversely, the structure-specific binding property of biomolecules has been used to sort carbon nanotubes of different kinds.<sup>12</sup> Despite such applications, a fundamental knowledge of the interactions of biomolecules with inorganic nanomaterials is scarcely limited. In order to fully capitalize on the novel properties of nanobio conjugates, a detailed understanding of the nature, physical and chemical mechanisms, structure, and spatial distribution of the conjugating molecules and nanomaterials is critically important.

Recently, a number of first-principles quantum chemical studies have focused on determining the site-specificity/selectivity of the biomolecular reactions with nanostructured materials. In the case of nucleobases of DNA and RNA, it has been shown that the N-site is the preferred site for forming a stable bioconjugate complex with metallic<sup>13</sup> and semiconducting quantum dots.<sup>14</sup> A considerable charge transfer occurs from nucleobases to metallic cluster, suggesting the dominance of electrostatic interaction in metal conjugates, while covalent interactions dominate the interaction in semiconducting conjugates. On the

other hand, interactions of tubular configurations of carbon and boron nitride with nucleobases of DNA and RNA have been shown to mainly result from van der Waals (vdW) interactions, whose strength depends on individual polarizability of nucleobases.<sup>15,16</sup>

As proteins play one of the most important roles in biology, it is expected that a similar understanding of their interactions with nanomaterials, as for DNA, would provide critical fundamental knowledge on their interactions and possibly be a guide for utilizing nanotechnology in proteomics. Toward that, recently, a number of studies have focused on carbon-based nanostructures,<sup>11,17–23</sup> addressing the challenges to interface proteins with nanomaterials.<sup>24</sup>

Boron nitride nanotubes (BNNTs), which possess a similar morphology as carbon nanotubes (CNTs) but distinct properties of their own, appear to be potential candidates for biomedical applications due to their uniformity and stability in dispersion in solution.<sup>25</sup> Unlike CNTs, whose electronic structure and properties vary widely based upon tube helicity, concentric layers, and so forth, the BNNTs are semiconducting regardless of their diameter and chirality.<sup>26</sup> BNNTs are also found to be nontoxic to health and environment due to their chemical inertness and

**Received:** August 3, 2011

**Accepted:** September 6, 2011

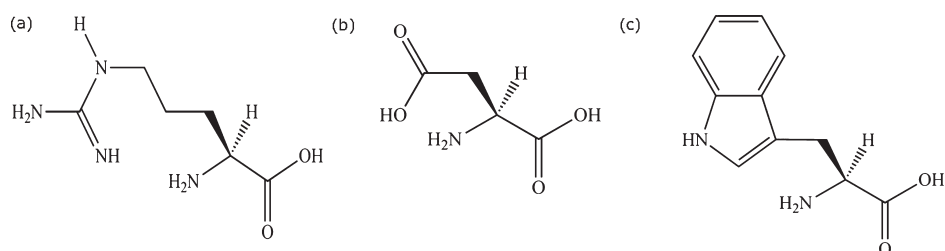


**Figure 1.** Chemical formulas of the studied amino acid molecules (a) Arg, (b) Asp, and (c) Trp.

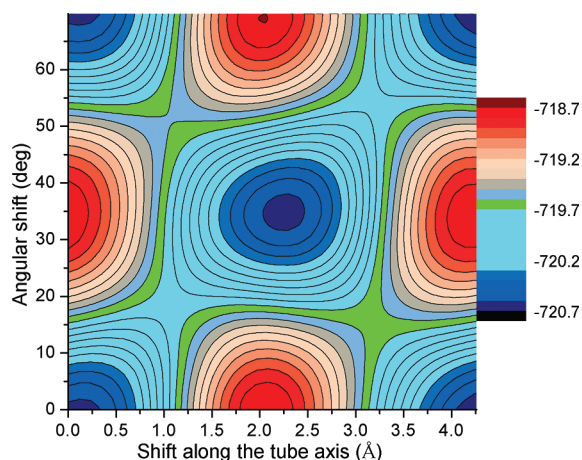


**Figure 2.** The calculated potential energy surface of arginine scanning tubular surface of BNNT. The energy barrier between two adjacent local minima is 1.5 eV.

structural stability, and therefore, they are more suitable for medical applications such as drug delivery.<sup>27,28</sup>

Toward that, we have performed first-principles quantum chemical calculations on the conjugation and electronic structure nature of amino acids, the building blocks of proteins, and BNNT. In principle, a complete understanding of the physics and chemistry of the interaction between the amino acid and BNNT should include an investigation of all 20 amino acid molecules interacting with BNNTs. However, it would have been prohibitively computationally expensive, particularly with the level of accuracy that we employed to obtain the optimized configurations of the bioconjugates involving all amino acids. Instead, we considered three representative molecules belonging to all three prevalent classes, such as, aspartic acid (Asp), a dicarboxylic amino acid with a negative charge, arginine (Arg), a three-carbon aliphatic chain with a positively charged guanidino group, and tryptophan (Trp), a nonpolar aromatic amino acid consisting of an indole functional group with an amine (Figure 1). We speculate that the nature of interaction of BNNTs with these representative amino acid molecules will be similar to that of the other amino acid molecules falling under the same category depending on their individual polarity, qualitatively. This choice of polar and nonpolar amino acids is expected to reflect the common chemical properties of more complex protein macromolecules. Thus, the present study will be useful in understanding how the polarity of the individual amino acid affects its interaction with BNNT.

In the energy surface scan plot obtained in the optimization step (ii) (please see Computational Methods for a detailed description)

shown in Figure 2, a striking difference between the interaction of BNNT with the amino acid molecules and that with the nucleobases of DNA and RNA<sup>16</sup> is revealed. For Arg-BNNT, the energy barrier between two adjacent minima is predicted to be significantly higher than what was reported for guanine-BNNT.<sup>16</sup> The molecular interaction of the Arg-conjugated BNNT therefore appears to be stronger than those in the nucleobase-conjugated BNNT. Figure 3 shows the equilibrium configurations of Asp-BNNT, Arg-BNNT, and Trp-BNNT complexes. It is interesting to note that Trp, the charge-neutral amino acid molecule, gets adsorbed on BNNT with its five- and six-membered rings almost parallel to the surface of the tube. However, it does not follow a perfect Bernal's AB stacking as reported in earlier calculations for the neutral DNA/RNA nucleobases on the surface of BNNT.<sup>16</sup>

The interatomic separation of the individual atoms of the amino acid molecules from the atoms of the tubular surface in the equilibrium configuration is plotted in Figure 4. The minimum  $R_{\text{amino-BNNT}}$  is 1.6, 2.01, and 2.87 Å for Arg, Asp, and Trp, respectively. The minimum  $R_{\text{Trp-BNNT}}$  is comparable to the separation calculated for neutral nucleobases (2.77 Å)<sup>16</sup> and organic molecules (2.96 Å)<sup>29</sup> physisorbed on BNNTs. The minimum  $R_{\text{Arg-BNNT}}$  is comparable to the intermediate distance between BNNT and chemisorbed amino functional groups  $\text{NH}_2\text{CH}_3$ ,  $\text{NH}_2\text{CH}_2\text{OCH}_3$ , and  $\text{NH}_2\text{CH}_2\text{COOH}$  (1.74, 1.76, and 1.77 Å, respectively).<sup>30</sup> On the other hand, the minimum  $R_{\text{Asp-BNNT}}$  is nearly the same as that calculated for  $\text{NH}_2\text{COOH}$  and BNNT (2.32 Å).<sup>30</sup> It therefore appears that the structural parameters of the ground-state configurations depend strongly on the nature of the side groups when adsorbed on the BNNTs, though the amino-functional group is present in all cases.<sup>30</sup>

The predicted difference for  $R_{\text{amino-BNNT}}$  of the Arg-BNNT and Asp-BNNT complexes, in a way, provides guidance to differentiate the nature of the interaction regimes in the bioconjugates considered.<sup>31</sup> For example, the minimum  $R_{\text{Trp-BNNT}}$  of 2.87 Å is similar to the characteristic distance for vdW-bound systems<sup>32</sup> where  $\pi$ -electrons associated with the indole functional group of Trp facilitate noncovalent interactions with the tubular surface of boron nitride.

The binding energy of the amino acid-conjugated BNNT was calculated using the asymptotic limit, moving the amino acid molecule away from the surface along the direction perpendicular to the tubular axis of the BNNT to the point beyond which the interaction between amino acid and BNNT becomes negligible (Figure 5). The calculated binding energy is 3.53, 0.94, and 0.36 eV for Arg-BNNT, Asp-BNNT, and Trp-BNNT, respectively (Table 1). The interaction strength therefore depends on the chemical nature of the side groups within the molecules themselves; the polar Arg and Asp molecules have a higher binding energy than the nonpolar aromatic Trp. It is worth noting that the same hierarchy of the order of the binding energy was obtained for a

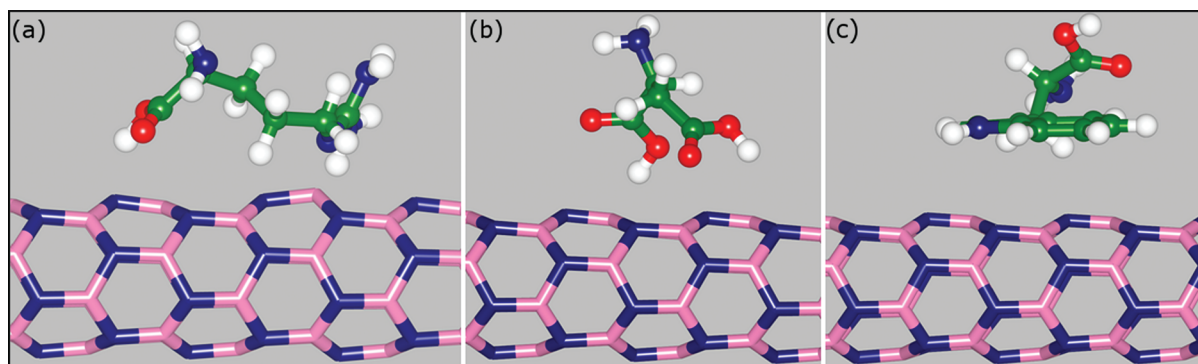


Figure 3. Equilibrium geometry of (a) Arg, (b) Asp, and (c) Trp on the surface of the BNNT.

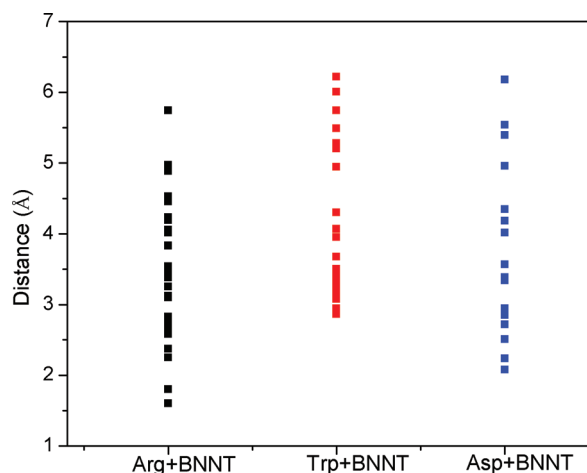


Figure 4. The distance between the atoms of the amino acid molecules and the tubular surface atoms in the equilibrium configurations of BNNT conjugates.

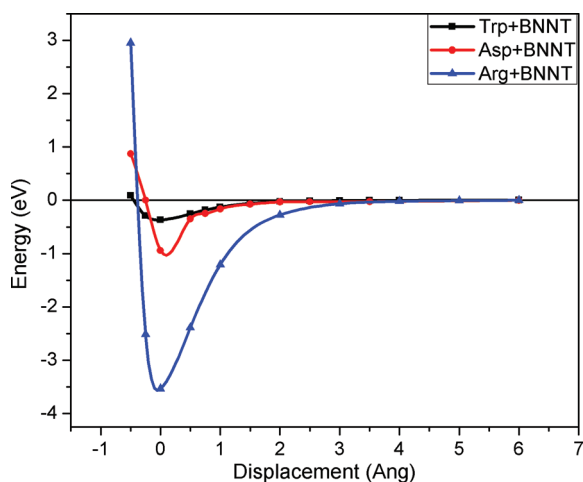


Figure 5. The potential energy variation of the amino acid molecules interacting with the BNNT as a function of the distance. Zero of the energy is aligned to the noninteracting regime of the surface. Zero of displacement represents the equilibrium configuration of the conjugated system.

metallic (5,5) CNT,<sup>17</sup> though the range is much smaller than that of conjugated BNNT complex. The binding energies of the conjugated

Table 1. Nearest-Neighbor Distance ( $R_{\text{amino-BNNT}}$ ), Binding Energy, and Band Gap of Amino-Acid-Conjugated BNNT

system	$R_{\text{amino-BNNT}}$ (Å)	binding energy (eV)	band gap (eV)
Arg-BNNT	1.6	3.53	2.2
Asp-BNNT	2.1	0.94	2.1
Trp-BNNT	2.9	0.36	1.6

CNT complexes are reported to be 0.46, 0.19, and 0.16 eV for Arg-CNT, Asp-CNT, and Trp-CNT, respectively. Previously, (7,7) BNNTs were also anticipated to bind with one of the amino acid molecules (alanine) rather strongly as compared to (7,7) CNTs.<sup>23</sup> The semiconducting BNNTs are therefore predicted to be more sensitive toward amino acid molecules, having higher distinction ability relative to that of CNTs. Furthermore, the presence of polar bonds and an intrinsic dipole moment indicates the possibility of using BNNTs as a more efficient protein immobilizer compared to CNTs.

Here, we find an important relevance of this study on the protein chemistry. Previously, the proteins were reported to get physisorbed on the CNTs<sup>3</sup> by weak dispersive forces whereas BNNTs were found to immobilize the proteins through the electrostatic interactions between the BNNT and the bound amino groups<sup>33</sup> because of the intrinsic polar bonds present in BNNTs. Interestingly, the amino acid molecules considered in this study exhibit similar preference as far as the binding to the CNTs<sup>17</sup>/BNNTs is concerned. It is therefore conclusive enough to claim that the individual amino acid molecules retain their interaction properties even when interacting with CNTs/BNNTs as a part of a protein. The stronger binding of the proteins with the BNNTs may often be seen as a potential source of toxicity; however, BNNTs are known to be nontoxic<sup>27,28</sup> so far. On the other hand the enhanced protein stability by BNNTs may, consequently, be utilized toward the enzyme degradation and to increase the activity via immobilization at the surface of the tube.<sup>34</sup>

In order to understand the effect of the adsorption of the molecules on the electronic properties of pristine BNNT, total density of the states (DOS) was calculated (not shown here). No significant change in the characteristic features of the DOS was seen for Asp- and Arg-conjugated BNNT relative to that of the pristine BNNT. It resembles the “harmless modification” observed in chemisorbed amino-functional conjugates on BNNT.<sup>30</sup> The LDA-DFT value of the band gap of the pristine (5,0) BNNT is 2.2 eV, whereas, the experimental value of the band gap of BNNT is about 5.5 eV.<sup>35</sup> For Trp-BNNT, the band gap is, however, drastically



reduced to 1.6 eV, indicating a significant change due to its noncovalent functionalization with Trp. The top of the valence band is associated with the *N*-2p orbitals of BNNT in both polar complexes. This is in contrast to the case of Trp-BNNT, where reduction of the band gap is predicted due to appearance of an additional peak near the Fermi level. Interestingly, the projected density of states shown in Figure 6 attributes this peak (forming the top of the valence band) to the Trp p-orbitals, though the nature of the bottom of the conduction band remains the same as that of the pristine BNNT. This is an indirect confirmation of the weak vdW interaction describing the Trp-BNNT conjugated system. The individual valence bands of Trp and BNNT appear to be unaltered in the Trp-BNNT complex, unlike the cases with Asp- and Arg-conjugated systems where the top of the valence band consists of hybrid states from Asp or Arg along with the BNNT. A similar trend was reported in recent literature where band gap modification was predicted for neutral nucleobase molecules when physisorbed onto BNNTs with vdW interaction,<sup>16</sup> and no reduction in the band gap of the BNNT was noted when the interaction was ionic.<sup>30</sup>

It is worth mentioning here that Trp is also known as a protein fluorophore due to the fact that the fluorescence of a protein is governed by the Trp residue. Its optical transitions, absorption at 280 nm and fluorescence at 348 nm, are associated with electronic transitions of the indole functional group (Figure 1).

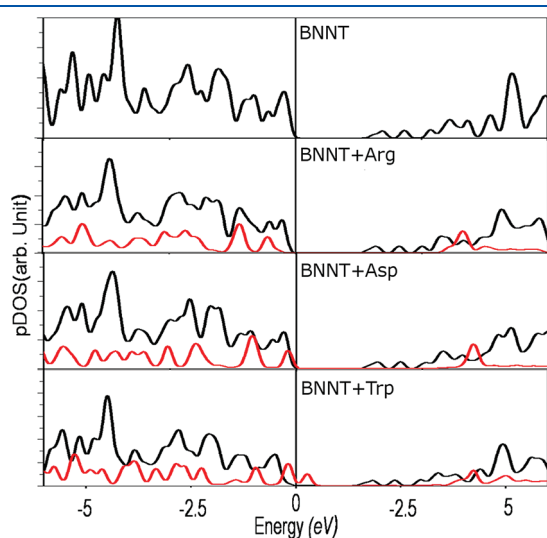


**Figure 6.** Projected density of states of pristine BNNT and amino acid conjugated BNNT. The black lines represent contributions from BNNT atoms, and the red lines refer to contribution from atoms of the amino acid molecules.

A quenching of the Trp fluorescence in the Trp-BNNT complex is therefore predicted, similar to the case predicted for the Trp-ZnO complex.<sup>36</sup>

A Bader charge analysis was performed to obtain the atomic charges of the ground-state configurations of bioconjugates. Negligible charge transfer was found for Trp-BNNT, while the polar complexes showed some charge transfer; for example, in Arg-conjugated BNNT, a charge of 0.15e was transferred from B of BNNT to N of Arg at a distance of 1.6 Å. Because  $R_{\text{Arg-BNNT}}$  is smaller than  $R_{\text{Asp-BNNT}}$  (Figure 4), the large difference in the binding energies (Table 1) of Arg-BNNT and Asp-BNNT complexes can be understood in terms of electrostatic interactions as the Coulomb potential varies inversely proportionally with the distance between the interacting entities. The results of the Bader charge analysis are further reaffirmed by Figure 7 showing a relatively large overlap of the electron clouds of Arg and BNNT compared to the cases of Asp-BNNT and Trp-BNNT. The strong attachment of the amino acid molecules onto the BNNTs by means of a charge-transfer mechanism was observed to be the key factor for the isolation of individual BNNTs via peptide wrapping<sup>37</sup> in recent experiments. The strong binding of Arg, and possibly the other positively charged amino acid molecules, onto the BNNTs with a significant charge transfer is perhaps the origin of the experimentally observed natural affinity of a protein toward BNNTs.<sup>33</sup> This enables the BNNTs to immobilize the proteins directly, without the use of any additional coupling reagent.<sup>33</sup>

Covalent functionalization of multiwalled BNNTs was achieved<sup>38</sup> using organic functional groups, naphthoyl chloride ( $\text{C}_{10}\text{H}_7\text{COCl}$ ), butyryl chloride ( $\text{CH}_3(\text{CH}_2)_2\text{COCl}$ ), and stearoyl chloride ( $\text{CH}_3(\text{CH}_2)_{16}\text{COCl}$ ). It was shown that these functional groups act as dopants in the BNNT, introducing additional gap states due to charge transfer between the functional groups and BNNT.<sup>38</sup> This is not the case for the amino acid-BNNT complexes considered. The polar amino acids Asp and Arg do not introduce any additional states in the band gap of the pristine BNNT, though charge transfer occurs in the bioconjugated complex.

Combining the results of structural configuration, binding energy, and analysis of atomic charges and electron density, we may therefore conclude that the nonpolar Trp molecule gets physisorbed whereas the polar Arg and Asp molecules are bound to the tubular surface of BNNT by electrostatic interactions. A relatively large binding energy of the Arg-BNNT complex may suggest the possibility of Arg being the amino acid that can facilitate a direct link to the tubular surface of BNNT.

In summary, we have investigated the interaction of a small-diameter BNNT with three amino acid molecules of different polarities. For the neutral Trp molecule, the interaction is found

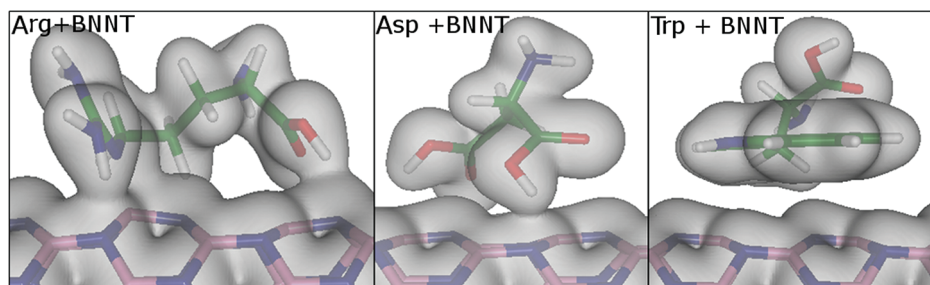


**Figure 7.** Total charge density of amino acid conjugated BNNT. The isosurface levels were set at 0.02 e/bohr<sup>3</sup> for all of the cases.

to be mediated by vdW forces. For the polar Arg and Asp molecules, the interaction seems to be mainly governed by electrostatic forces. A large variation in the magnitude of binding energy in these bioconjugated complexes suggests a higher electronic sensitivity of semiconducting BNNTs relative to metallic CNTs for amino acids of different polarities, leading to possible applications of BNNTs in protein immobilization. The predicted stronger attachment of Arg, and possibly the other positively charged amino acid molecules, with the BNNTs explains the experimentally observed natural affinity of a protein toward BNNTs and thereby enables the BNNTs to immobilize the proteins without any additional coupling reagent. Additionally, the insights gained from this theoretical study are expected to assist in the future development of BNNTs with targeted chemoselectivity via suitable chemical functionalization. Calculations are currently in progress with oligopeptides consisting of amino acids to understand the role of neighboring amino acids in determining the nature of interaction for the conjugated BNNT.

## ■ COMPUTATIONAL METHODS

In the calculations, a plane-wave pseudopotential approach within the local density approximation (LDA) of density functional theory was employed using the Vienna ab initio simulation package (VASP). A  $1 \times 1 \times 3$  Monkhorst–Pack grid<sup>39</sup> was used for *k*-points sampling of the Brillouin zone with an energy cutoff of 850 eV. The cutoff criterion for the force gradient was set as 0.03 eV Å<sup>-1</sup>. The supercell considered for electronic structure calculations consisted of a (5,0) single-walled BNNT<sup>40</sup> with a diameter of 4.16 Å. Because the amino acid molecules were set to approach the BNNT along the *x*-axis (perpendicular to the tube axis of the BNNT that is parallel to the *z*-axis) with different orientations, a large vacuum distance (~32 Å) was given in the *x*-direction to avoid the unphysical interaction of the repeating units, whereas a separation of 15 Å was given along the *y*-axis. The system is periodic in the *z*-axis (i.e., along the tube axis) to simulate an infinitely long BNNT. The average B–N bond length in the optimized configuration of the pristine BNNT is 1.44 Å, in agreement with a first-principles DFT calculations.<sup>29</sup>

Although, the LDA-DFT level of theory may not be the optimal choice for calculating interaction energies of weakly bound systems represented by vdW interactions, recent theoretical studies<sup>41</sup> considering adsorption of adenine on graphite have shown that the topology of the potential energy surface obtained by this method remains effectively indistinguishable from the one obtained using the more sophisticated generalized gradient approximation (GGA)<sup>42</sup> together with a modified version of the London dispersion formula for vdW interactions. Also, there are some cases where LDA has been shown to yield a better description of the weakly bound systems compared to the GGA, which fails to predict binding in otherwise vdW-bound systems.<sup>43,44</sup> As a viable remedy toward the present investigation of biomolecules of different polarities where their interactions with BNNT might deviate from vdW forces, we used the LDA-DFT level of theory and followed the asymptotic approach to calculate the binding energy of a bioconjugated complex. It is expected that a possible cancellation of errors might qualitatively retain the relative trend, and thereby, the basic underlying physics and chemistry governing the interaction of amino acid molecules with BNNT should be unaltered. However, it is noteworthy that because the LDA-DFT underestimates the band gap of the

systems, discussions on the band gap of all of the systems considered in this study are, therefore, qualitative.

We begin with individually optimized configurations of BNNT and the amino acid molecules and perform the following steps to obtain the equilibrium configuration of the bioconjugated system: (i) Selective dynamics: An initial force relaxation calculation step to determine the preferred orientation and optimum height of the amino acid molecules relative to the tubular surface. (ii) Grid scan: The energy surface is obtained by translating the relaxed amino acid molecules parallel to the BNNT surface covering a surface area 4.26 Å in height and 70° in angular range and containing a mesh of 230 scan points (Figure 2). The separation between the molecule and the tubular surface is held fixed at the optimum height determined in step (i). (iii) Rotation: Considering the nonplanar structures of the amino acid molecules, we investigate a number of different orientations for how the molecules might possibly prefer to approach the side wall of BNNT. (iv) Full optimization: A full optimization of the conjugated system starting from the lowest-energy configuration obtained in the previous steps. In this step, both the BNNT and amino acid molecule are free to relax. It is worth noting that a similar optimization procedure has been applied successfully on carbon and boron nitride nanostructures interacting with nucleobases of DNA and RNA by our research group.<sup>15,16</sup>

## ■ AUTHOR INFORMATION

### Corresponding Author

\*E-mail: pandey@mtu.edu. Address: Department of Physics, Michigan Technological University, 1400 Townsend Drive, Houghton, MI 49931-1295. Phone: 906-487-2086 (R.P.); E-mail: Shashi.p.karna.civ@mail.mil. Phone: 410-306-0723 (S.P.K.).

## ■ ACKNOWLEDGMENT

Helpful discussions with Sankara Gowtham are thankfully acknowledged. The work at Michigan Technological University was performed under support by the Army Research Office through Contract Number W911NF-09-1-0221. R.H.S. thanks the Swedish Research Council (VR, Grant No. 621-2009-3628) for financial support.

## ■ REFERENCES

- (1) Chen, R. J.; Bangsaruntip, S.; Drouvalakis, K. A.; Kam, N. W. S.; Shim, M.; Li, Y. M.; Kim, W.; Utz, P. J.; Dai, H. J. *Proc. Natl. Acad. Sci. U.S.A.* **2003**, *100*, 4984.
- (2) Chen, R. J.; Zhang, Y. G.; Wang, D. W.; Dai, H. J. *J. Am. Chem. Soc.* **2001**, *123*, 3838.
- (3) Kang, Y.; Liu, Y. C.; Wang, Q.; Shen, J. W.; Wu, T.; Guan, W. J. *Biomaterials* **2009**, *30*, 2807.
- (4) Pantarotto, D.; Partidos, C. D.; Graff, R.; Hoebeke, J.; Briand, J. P.; Prato, M.; Bianco, A. J. *Am. Chem. Soc.* **2003**, *125*, 6160.
- (5) Wong, S. S.; Joselevich, E.; Woolley, A. T.; Cheung, C. L.; Lieber, C. M. *Nature* **1998**, *394*, 52.
- (6) Cui, Y.; Wei, Q. Q.; Park, H. K.; Lieber, C. M. *Science* **2001**, *293*, 1289.
- (7) Benyamini, H.; Shulman-Peleg, A.; Wolfson, H. J.; Belgorodsky, B.; Fadeev, L.; Gozin, M. *Bioconjugate Chem.* **2006**, *17*, 378.
- (8) Hong, R.; Fischer, N. O.; Verma, A.; Goodman, C. M.; Emrick, T.; Rotello, V. M. *J. Am. Chem. Soc.* **2004**, *126*, 739.
- (9) You, C. C.; Agasti, S. S.; De, M.; Knapp, M. J.; Rotello, V. M. *J. Am. Chem. Soc.* **2006**, *128*, 14612.
- (10) Staii, C.; Johnson, A. T. *Nano Lett.* **2005**, *5*, 1774.
- (11) Heller, D. A.; Jeng, E. S.; Yeung, T. K.; Martinez, B. M.; Moll, A. E.; Gastala, J. B.; Strano, M. S. *Science* **2006**, *311*, 508.

- (12) Tu, X. M.; Manohar, S.; Jagota, A.; Zheng, M. *Nature* **2009**, *460*, 250.
- (13) Soto-Verdugo, V.; Metiu, H.; Gwinn, E. J. *Chem. Phys.* **2010**, *132*, 195102.
- (14) Shewale, V.; Joshi, P.; Mukhopadhyay, S.; Deshpande, P.; Pandey, R.; Hussain, S.; Karna, S. P. *J Phys. Chem. C* **2011**, *115*, 10426.
- (15) Gowtham, S.; Scheicher, R. H.; Pandey, R.; Karna, S. P.; Ahuja, R. *Nanotechnology* **2008**, *19*, 125701.
- (16) Mukhopadhyay, S.; Gowtham, S.; Scheicher, R. H.; Pandey, R.; Karna, S. P. *Nanotechnology* **2010**, *21*, 165703.
- (17) Chang, C. M.; Jalbout, A. F. *Thin Solid Films* **2010**, *518*, 2070.
- (18) Cveticanin, J.; Joksic, G.; Leskovic, A.; Petrovic, S.; Sobot, A. V.; Neskovic, O. *Nanotechnology* **2010**, *21*, 015102.
- (19) Gan, L. B.; Zhou, D. J.; Luo, C. P.; Tan, H. S.; Huang, C. H.; Lu, M. J.; Pan, J. Q.; Wu, Y. J. *Org. Chem.* **1996**, *61*, 1954.
- (20) Rajesh, C.; Majumder, C.; Mizuseki, H.; Kawazoe, Y. *J. Chem. Phys.* **2009**, *130*, 124911.
- (21) Sun, W. M.; Bu, Y. X.; Wang, Y. X. *J. Phys. Chem. B* **2008**, *112*, 15442.
- (22) Vardanega, D.; Picaud, F. *J. Biotechnol.* **2009**, *144*, 96.
- (23) Zheng, J. X.; Song, W.; Wang, L.; Lu, J.; Luo, G. F.; Zhou, J.; Qin, R.; Li, H.; Gao, Z. X.; Lai, L.; Li, G. P.; Mei, W. N. *J. Nanosci. Nanotechnol.* **2009**, *9*, 6376.
- (24) Kane, R. S.; Stroock, A. D. *Biotechnol. Prog.* **2007**, *23*, 316.
- (25) Yu, J.; Chen, Y.; Cheng, B. M. *Solid State Commun.* **2009**, *149*, 763.
- (26) Chopra, N. G.; Luyken, R. J.; Cherrey, K.; Crespi, V. H.; Cohen, M. L.; Louie, S. G.; Zettl, A. *Science* **1995**, *269*, 966.
- (27) Chen, X.; Wu, P.; Rousseas, M.; Okawa, D.; Gartner, Z.; Zettl, A.; Bertozzi, C. R. *J. Am. Chem. Soc.* **2009**, *131*, 890.
- (28) Cohen, M. L.; Zettl, A. *Phys. Today* **2010**, *63*, 34.
- (29) Akdim, B.; Kim, S. N.; Naik, R. R.; Maruyama, B.; Pender, M. J.; Pachter, R. *Nanotechnology* **2009**, *20*, 8.
- (30) Wu, X. J.; An, W.; Zeng, X. C. *J. Am. Chem. Soc.* **2006**, *128*, 12001.
- (31) Grabowski, S. J.; Sokalski, W. A.; Dyguda, E.; Leszczynski, J. *J. Phys. Chem. B* **2006**, *110*, 6444.
- (32) Watson, J. D.; Baker, T. A.; Bell, S. P.; Gann, A.; Levine, M.; Losick, R. *Molecular Biology of the Gene*; 5th ed.; Benjamin Cummings: San Francisco, CA, 2004.
- (33) Zhi, C.; Bando, Y.; Tang, C.; Golberg, D. *J. Am. Chem. Soc.* **2005**, *127*, 17144.
- (34) Lynch, I.; Dawson, K. A. *Nano Today* **2008**, *3*, 40.
- (35) Lauret, J. S.; Arenal, R.; Ducastelle, F.; Loiseau, A.; Cau, M.; Attal-Tretout, B.; Rosencher, E.; Goux-Capes, L. *Phys. Rev. Lett.* **2005**, *94*, 037405.
- (36) Joshi, P.; Shewale, V.; Pandey, R.; Shanker, V.; Hussain, S.; Karna, S. P. *Phys. Chem. Chem. Phys.* **2011**, *13*, 476.
- (37) Gao, Z. H.; Zhi, C. Y.; Bando, Y.; Golberg, D.; Serizawa, T. *J. Am. Chem. Soc.* **2010**, *132*, 4976.
- (38) Zhi, C. Y.; Bando, Y.; Tang, C. C.; Golberg, D. *Phys. Rev. B* **2006**, *74*, 153413.
- (39) Monkhorst, H. J.; Pack, J. D. *Phys. Rev. B* **1976**, *13*, 5188.
- (40) Xiang, H. J.; Yang, J. L.; Hou, J. G.; Zhu, Q. S. *Phys. Rev. B* **2003**, *68*, 035427.
- (41) Ortmann, F.; Schmidt, W. G.; Bechstedt, F. *Phys. Rev. Lett.* **2005**, *95*, 186101/1.
- (42) Perdew, J. P.; Chevary, J. A.; Vosko, S. H.; Jackson, K. A.; Pederson, M. R.; Singh, D. J.; Fiolhais, C. *Phys. Rev. B* **1992**, *46*, 6671.
- (43) Simeoni, M.; De Luca, C.; Picozzi, S.; Santucci, S.; Delley, B. *J. Chem. Phys.* **2005**, *122*, 214710.
- (44) Tournus, F.; Latil, S.; Heggge, M. I.; Charlier, J. C. *Phys. Rev. B* **2005**, *72*, 075431.